DESIGN PLAN OF SUPER MULTI-SPAN CONTINUOUS MENSHIN BRIDGE WITH DECK LENGTH OF 725 M

Hideji Masumoto*, Koji Hara, and Mikio Yamashita*****

***Director, Road Construction Division, Public Works Department, Shizuoko Prefectural Government**

****Assistant Chief, Construction Section 2, Numazu Public Works Office, Shizuoka Prefectural Government**

*****Director, Technical Department, KAIHATSU Consultant Co., Ltd. Higashiueno 2-9-4, Taitoku, Tokyo**

INTRODUCTION

The basic framework of the national highway system on Izu Peninsula in Shizuoka Prefecture is formed by Highway 135, which winds along the east coast of the Izu Peninsula, and Highways 136 and 414, which originate at Shimoda City and extend along the west coast of the peninsula to Mishima City. These highways contribute to development and tourism in Izu. Measures must be taken to deal with the traffic congestion that occurs on all parts of the peninsula as a result of the fact that most of the 80 million tourists and other travellers visit Izu Peninsula each year by car. As one measure to alleviate this problem, a 13.8 km stretch of highway is being built to smooth the flow of traffic in central Izu. One 5.2 km section on the Trans Izu Highway is a high-standard trunk road connecting Kannami-chou Tsukamoto to Shuzenji, where traffic congestion is particularly severe. The other section is an 8.6 km bypass on National Highway 136.

The Ohito Viaduct, with length of 1,929 m will be constructed in the Ohito-chou district of Tagata-gun in Shizuoka Prefecture as part of the high-standard trunk road (Trans Izu Highway) section of the above project (See Figure 1 and Photo 1).

This paper presents planning of this viaduct and describes the design plan of a super multi-span continuous Menshin bridge.

Photo 1. Location of the Ohito Viaduct Project

SUMMARY OF THE OHITO VIADUCT

The Ohito Viaduct, which will be constructed along the bank of the Kano River, will link the Kanogawa Interchange to the Ohito Interchange on the planned highway. This viaduct will consist of a series of five bridges. Table 1 Shows the bridge type adopted for each bridge.

From the beginning of the project, multi-span continuous bridges were planned to improve the maintainability and the road service standards. Bridge 2 is planned to be a 29-span continuous PC hollow-slab bridge with bridge length of 725 m, which will be the longest concrete bridge in Japan. Furthermore Menshin design is adopted for this bridge. A number of Menshin bridges have been constructed since 1991 when the Miyagawa Bridge which is the first Menshin bridge in Japan in Shizuoka Prefecture have been opened to traffic. Then the Menshin design is being widely applied for jointless measures for existing simply supported bridges. Furthermore, basic research on super multi-span continuous Menshin bridges, such as the Ohito Viaduct bridges, has been conducted as part of the "Joint Research Program on the Development of Menshin Systems for Highway Bridges", which is a joint government--private sector research project. As a result of this research, the super multi-span continuous Menshin bridge has been proposed as a highly feasible type of bridge, and studies are under way for its practical application. Before it can be applied to real bridges, solutions must be found to many unsolved problems. To prepare for the design work on these bridges, the basic design policies were established through the deliberation and guidance by the "Ohito Viaduct (Super multi-span Continuous Menshin Bridge) Committee of Inquiry" (Chairman: Dr. M. Fujiwara, Director of the Bridge and Structure Department, Public Works Research Institute, Ministry of Construction).

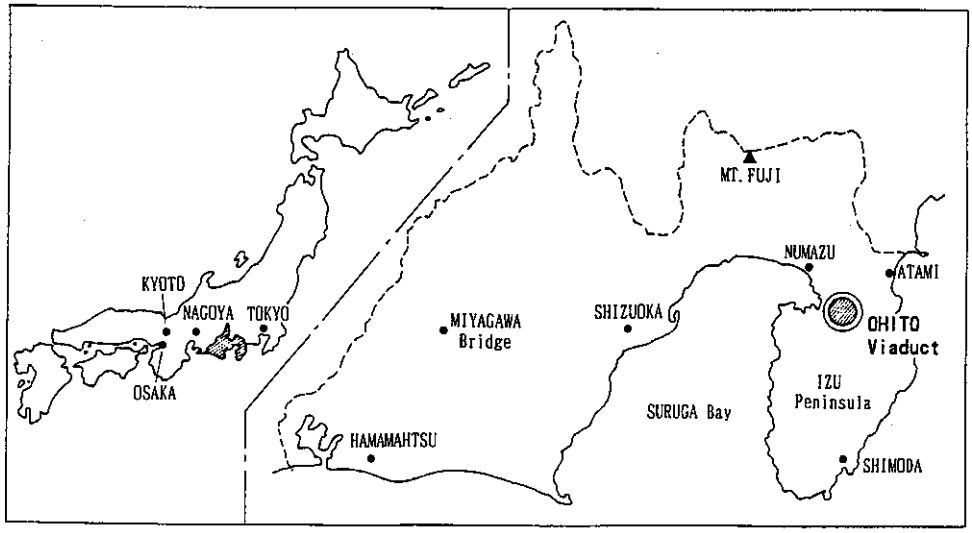

Figure 1. Location of the Ohito Viaduct

Table 1. Bridge Categories

Bridge 1	7-span continuous PC hollow slab bridge	L = 175.0m
Bridge 2	29-span continuous PC hollow slab bridge	L = 725.0m
Bridge 3	15-span continuous PC hollow slab bridge	L = 375.0m
Bridge 4	3-span continuous steel Box Girder bridge	L = 337.5m
Bridge 5	12-span continuous PC hollow slab bridge	L = 290.4m

STRUCTURAL DESIGN OF THE SUPER MULTI-SPAN CONTINUOUS MENSHIN BRIDGE

The following is a description of the structural design for bridge 2, which is the longest bridge in this viaduct project (See Figure 3).

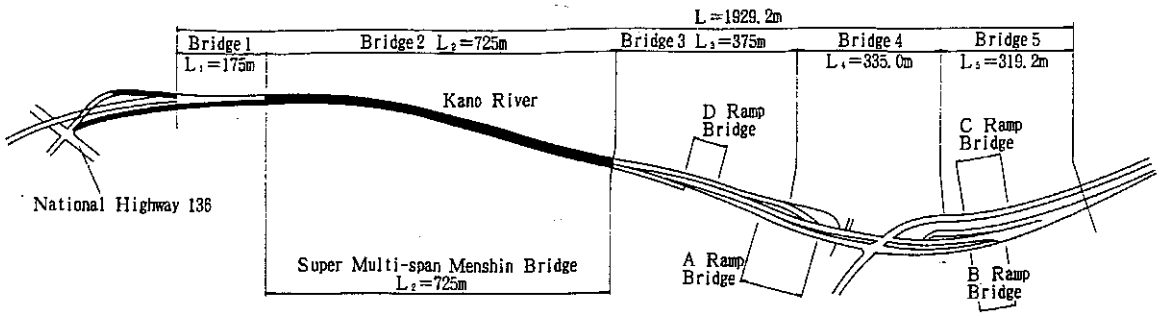

Figure 2. Plane View of the Ohito Viaduct

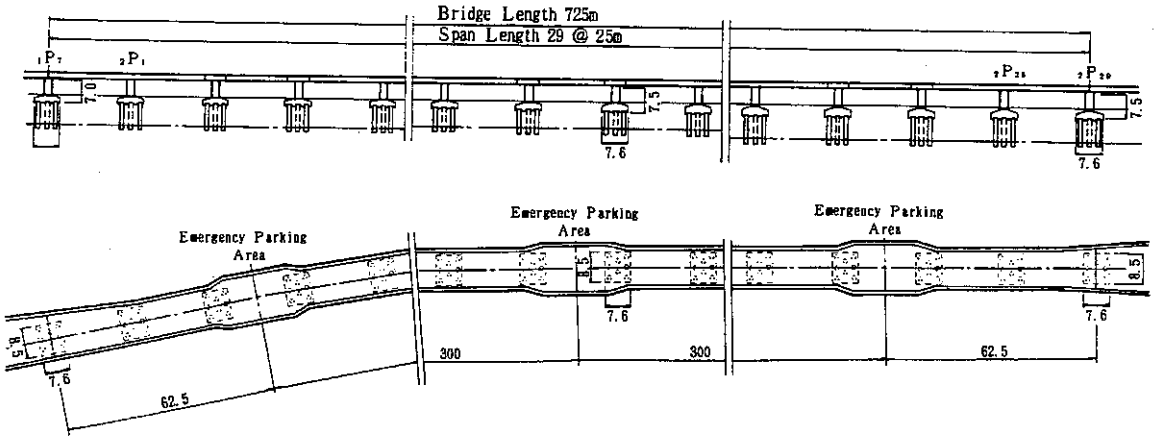

Figure 3. View of Bridge 2

1) Bridge Design conditions

*	Highway Standard	: 1 - 3
*	Design Vehicle Speed	: V = 80km/h
*	Width Configuration	: Total width W = 11.70 m (See Figure 4)
*	Effective Width	: We = 10.50 m (1.75m+3.50m+1.75m)
*	Cross section gradient:	: Standard 2.0%
*	Bridge Class	: First class bridge
*	Live Load	: TL-20, TT-43
*	Surface Material	: Asphalt paving V = 80 mm (design load thickness = 100 mm)
*	Handrail	: Concrete barrier curb (parapet) thickness = 300 mm
*	Noise barrier load	: W = 154.0 kgf/m
*	Ground condition	: Class 2

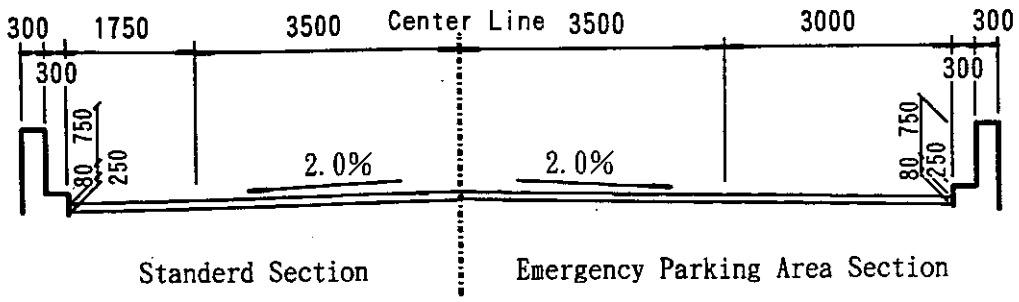

Figure 4. Cross Section of Roadway

2) Outline of the Ground

Figure 5 shows the structure of the strata in the cross longitudinal direction of the bridge based upon geological survey in the project area. A tertiary tuff stratum is found at approximately GL-40 m.The diluvium stratum above it consists of between 30 to 35 m of alternating strata of gravel, sand or clay layers. An alluvial gravel stratum Ag with N-value close to 50 is found near the surface. Initially this layer could be used as the supporting strata. However, the results of an on-site loading test conducted as part of a supplementary detailed geological survey showed that it would be difficult to rely on this as the supporting stratum. Accordingly, the underlying diluvial gravel strata Dq1 is planned to be the supporting stratum.

Table 2 shows the ground condition for the Menshin design, which is a key aspect of the bridge design. It is estimated as Class II through both the N-value and the shear wave velocity of the grounds.

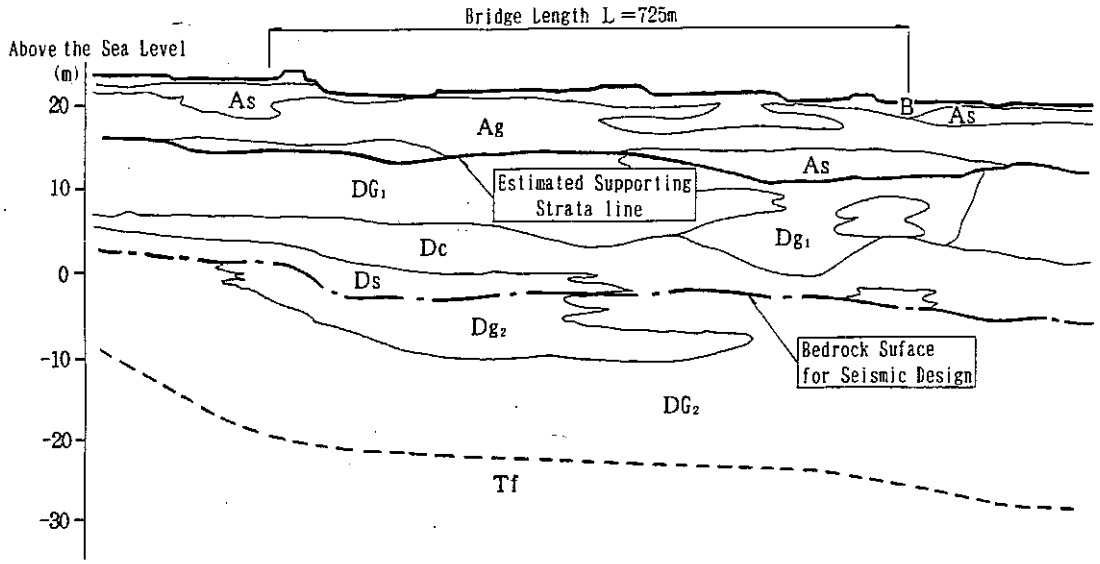

Figure 5. Longitudinal Diagram of the strata

Table 2. Ground Characteristic Value

Boring No.		Estimates Based on N-values		Computations Based on shear wave velocity	
		Ground Characteristic Value TG (sec)	Ground Class	Ground Characteristic Value TG (sec)	Ground Class
Prior Survey	H1−7	0.2≦0.328<0.6	Type II	——	——
	H2−6	0.2≦0.296<0.6	Type II	——	——
	H1−6	0.2≦0.588<0.6	Type II	——	——
New Survey	P4	0.2≦0.324<0.6	Type II	0.2≦0.245<0.6	Type II
	P19	0.2≦0.300<0.6	Type II	——	——
	P25	0.2≦0.316<0.6	Type II	0.2≦0.332<0.6	Type II
	P29	0.2≦0.352<0.6	Type II	——	——

3) Superstructure Design

(a) Structure Selection

The Type of superstructure is selected from among a range of structures determined by the restriction conditions described above. The span is determined by the crossing conditions, and the form of the superstructure was also restricted by the structural height. Consequently, a span length of 25 m was chosen. A PC hollow-slab bridge as the concrete girder type, and a multi-beam non-composite plate girder bridge as the steel girder type is selected for the comparison of bridge types. The conventional factors such as economic efficiency, structural properties, maintainability, harmony with adjoining sections, constructability, and environmental adaptability are considered, for the comparison, and their suitability for Menshin design and the thermal expansion and contraction properties of long girder were also considered.

Eventually PC continuous hollowslab bridges are selected .This bridge type is superior in terms of economic efficiency, continuity of the structure with that of the emergency parking areas, the integrated form of its superstructure and substructure, the stability of the Menshin bearing, and the expansion and contraction of the girder.

(b) Materials

* Concrete Strength : $\sigma_{ck} = 350 kgf/cm^2$
  $\sigma_{ck} = 210 kgf/cm^2$
* Reinforcing Bar : SD 295
* Prestressing Steel : SWPR 7 A 12T12.4
  SBPR 930/1180, Ø32mm

(c) Construction Method

Because this viaduct will be a 29-span continuous bridge, another prerequisite condition is that it must be constructed in separate sections. A study focused on the suitability for the site conditions, cost efficiency and the residual deformation during and after construction was conducted to determine specific type of construction method.

The use of a movable falsework is generally selected in the construction of a multi-span bridge in order to reduce labor requirements. However, a comparative study on partial construction using the support method showed that the support method was more cost efficient. Therefore, the support method was adopted as the basic construction method. Figure 6 shows residual deformation (drying shrinkage, creep deformation) according to the construction methods.

(d) Deformation of the Bearings and the Construction Method

In the case of this bridge, the residual deformation caused by the creep and drying shrinkage of PC girder will be as much as approximately 114.7 mm at the ends of the girder, even when a standard construction method is employed. Furthermore, the expansion and contraction of the girder under the effect of temperature change deformation will be ±75.2 mm. Figure 7 shows the deformation of the girder caused by creep, drying shrinkage and temperature change. On the one hand, if the bearings are simply designed to absorb these deformations, the thickness of the rubber of the bearings will increase, and the shearing stiffness of the bearings will decrease, resulted in the lengthening of the natural period. The displacement of the superstructure during an earthquake will also increase, and the design of ancillary structures will be influenced. For this reason, it is absolutely essential that one of two measures be adopted to deal with the residual deformation occurring in the superstructure. Either a reverse displacement is to be added when the bearings are manufactured in the factory, or else the deformation is to be corrected at site after the bearings are installed. Basic policies regarding these problems with the design of the bridge were laid out and all necessary studies were performed in the planning stage. Figure 8 shows the hypothetical range of bearing deformation. Because the method to add a reverse deformation to the bearings in the factory had already been used in a number of locations, the study was directed at deformation correction methods to be employed at site. Figure 9 shows a summary of the construction method proposed on the basis of this study.

Specific design detail and methods to be employed in the adoption of this method are now being studied, and plans call for additional experiments to be conducted and final decisions will be made by the time when the superstructure is constructed.

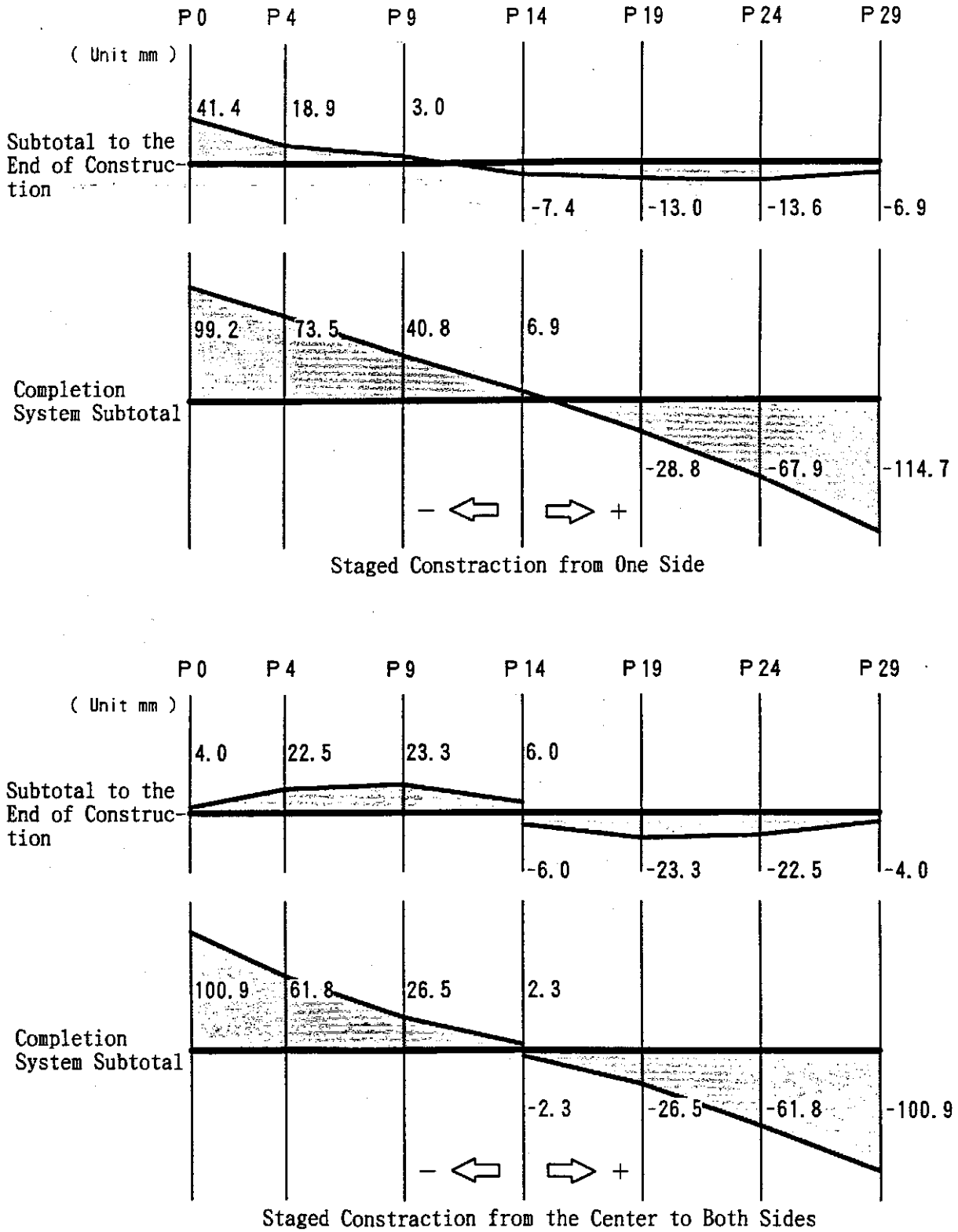

Figure 6. Residual Deformation Caused by Creep and Drying Shrinkage

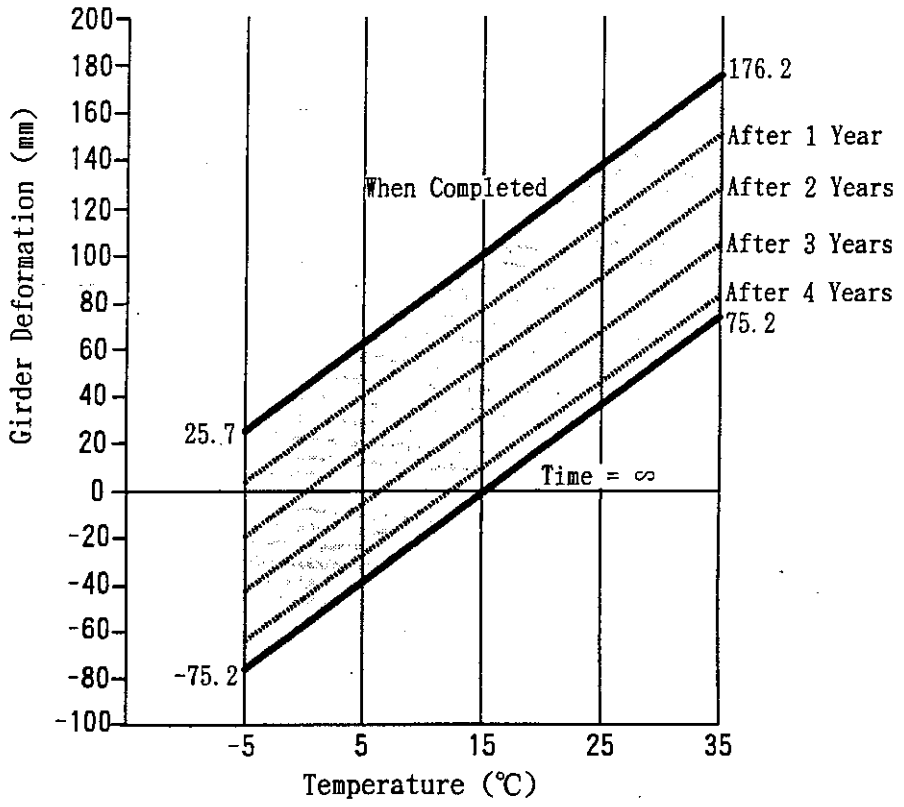

Figure 7. Deformation of Girder Caused by Creep, Drying Shrinkage, and Temperature Change

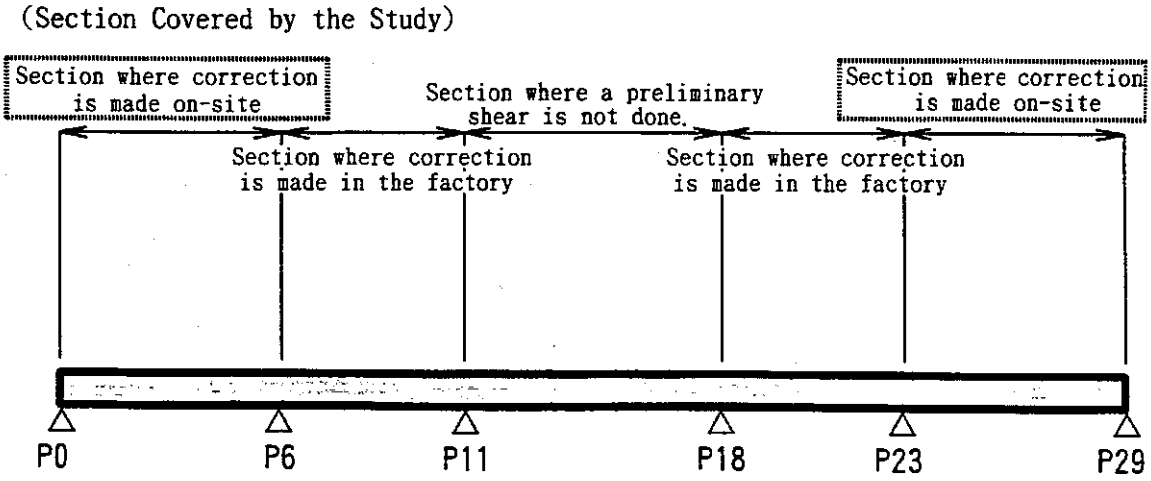

This scale, however, assumes the use of a conventional constraction method, and the range must be examined according to the condition.

Figure 8. Hypothetical Diagram of the Bearing Deformation Correction Range

① Ancher Bolt Installation

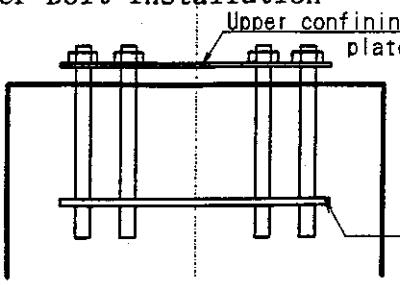

The ancher bolts fixed by the upper and lower confining plates, and the bridge pier concrete is placed

② Base Plate Installation

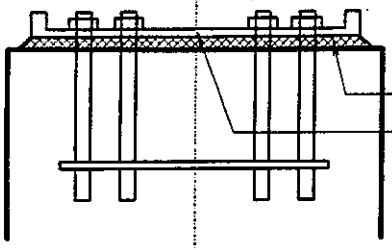

After the upper confining plate is removed, the base plate is set prescribed position, and schrinkage compensating mortar is placed.

③ Bearing(LRB) Installation and Placing Concrete for the Main Beam

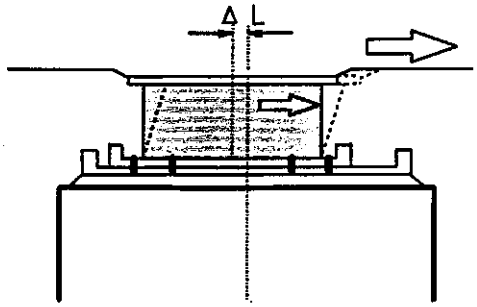

Only the deformation ΔL of the main beam is shifted, the bearing is set in place, and the main beam concrete is placed.

★The bottom plate and base plate are temporarily fixed in place with bolts at the temporarily installation location.

④ Post-strain Adjustment

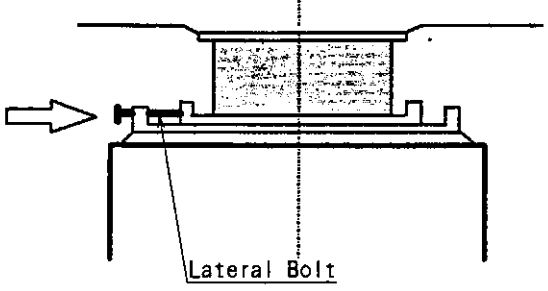

After the main beam is completed, post-strain adjustment is made with a horizontal bolts.

★It is necessary to perform staged post-strain adjustment at the ends.

★The use of a vertical jack to reduce the reaction force is being considered.

★Depending on the circum-stances, it is moved with a center-hole jack and fixed with a boltt.

⑤ Fixing the Lowar Plate and Base Plate

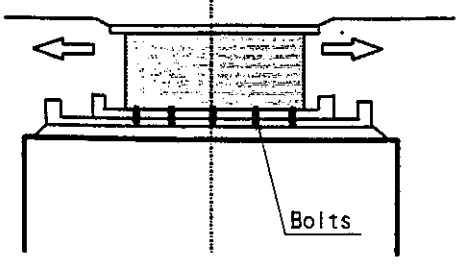

After post-strain adjustment has been completed, the bottom plate and base plate are fixed withe bolts.

★In a case when the movement and the error are large, the bottom plate and the base plate are fixed by welding

Figure 9. Proposed Bearing Deformation Correction Method

(e) Prestressing Steel Based on Statically Indeterminate force

As a result of residual deformation of the girder and temperature change deformation, additional axial force and moment act on the girder. These statically indeterminate forces is influenced by the stiffness of the Menshin bearings and by the stiffness of the bridge piers including the foundation. The deformation that occurs in the superstructure during construction and the residual deformation are dealt with separately. But the force generated by the expansion and contraction of the girder as a result of continuous temperature change deformation is a major factor because there are many supports and because of the long length of the girder. Figure 10 shows the thermal lateral force generated by Menshin bearings designed on the basis of one hypothesis and the results of computations of the axial force generated on the girder.

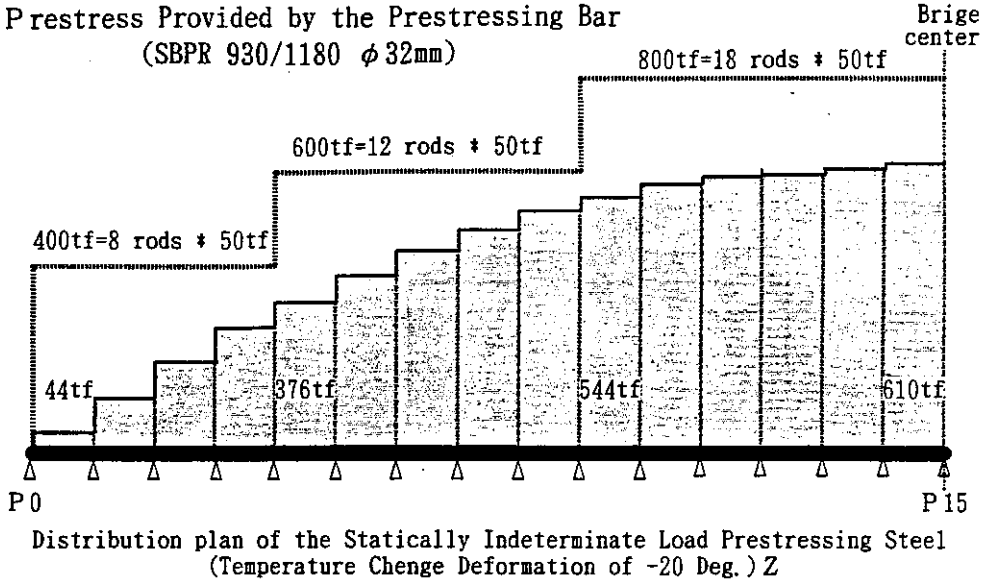

Figure 10. Axial Force Produced in the Girder by Temperature Change Deformation

Measures to deal with these statically indeterminate forces is examined. The best approach would be to handle the problem by installing prestressing bar (SBPR 930/1180) for statically indeterminate forces, which is in principle installed in the axial line of girder, in addition to prestressing cable (SWPR 7A-12T12.4) that handles the normal principle loads. Figure 11 shows the standard cross sections for the distribution of prestressing cable for principle loads and that for prestressing bar against statically indeterminate forces.

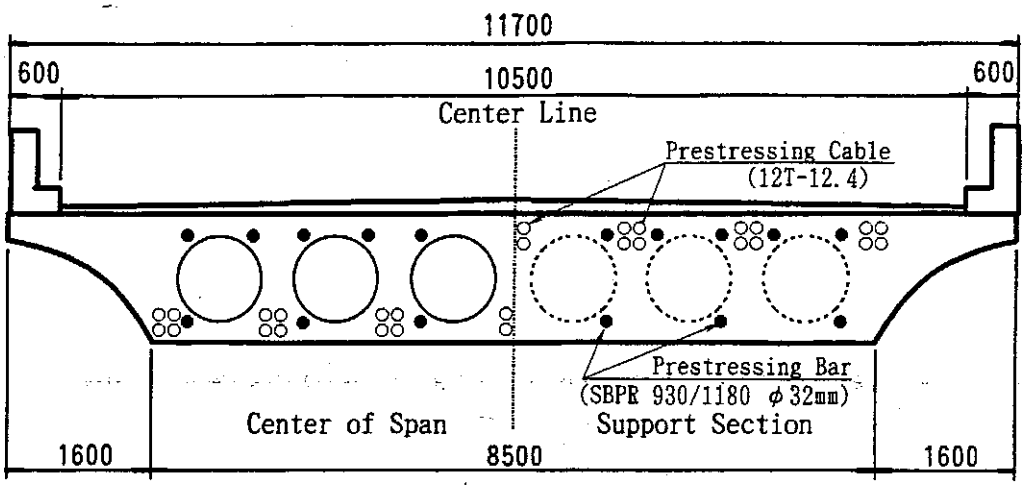

Figure 11. Distribution of Prestressing Steel in a Standard Cross Section

4) Design of the Substructure

(a) Design of the Shape

The bridge piers will be low, ranging from 7.0 m to 7.5 m high, since the longitudinal gradient is gentle, the ground at the site is flat, and pile foundation is employed. Ordinary walltype bridge piers will be selected, and their shape as shown in Figure 12 is employed in order to provide continuity with the cross section of the superstructure and to convey stability. To determine the shape of the substructure, three shapes compatible with the cantilever processing of the superstructure were compared and the one found to be visually superior was selected. Concerning the visual aspects in particular, the plan for the substructure of the entire viaduct varies from the basic single wall approach, to the substructure consist of two-column, or of a three-column rigid-frame type. Continuity among all sections was considered.

The wall thickness of intermediate piers other than end piers was found by simulating the volume of installed reinforcing bar, and carrying out a comprehensive comparison and assessment of thermal change deformation lateral forces, the lateral force of an L1 earthquake, the ultimate lateral strength during an L2 earthquake, based on the bridge pier stiffness in each case. The standard wall thickness was set at 2.0 m. Figure 13 shows the cross section of the bridge piers and the distribution of reinforcing bar.

(b) Materials

* Concrete : $\sigma_{ck} = 210 kgf/cm^2$
* Reinforcing Bar : SD 295 $\sigma_{sy} = 2{,}700 kgf/cm^2$

(c) Foundation

In the original plans, the direct foundation was placed on the gravel strata with N value between 40 and 50 found near the surface. However, the results of a later survey (including a plate bearing test) showed that this would be difficult, so the supporting layer was changed to the diluvial gravel found beneath it (Dg1).

Consequently, a pile foundation with length between 6 and 8 m was selected. Following a comparison of various types of piles, cast in place concrete piles (1,200 mm) are selected in consideration with bearing capacity efficiency, constructability, and cost efficiency.

(d) Substructure Stiffness

Table 3 shows an example of the computation of substructure stiffness, and Figure 14 shows the P-δ curve for the pier. Because the lateral reaction force caused by temperature change deformation is an important element in this design, when the spring constant of the pile foundation during a temperature change deformation is computed, it is assessed by the static normal spring of ground. The dynamic ground spring indicated in the Seismic Design of the highway bridge specifications is used as the ground spring constant during L1 and L2 earthquakes.

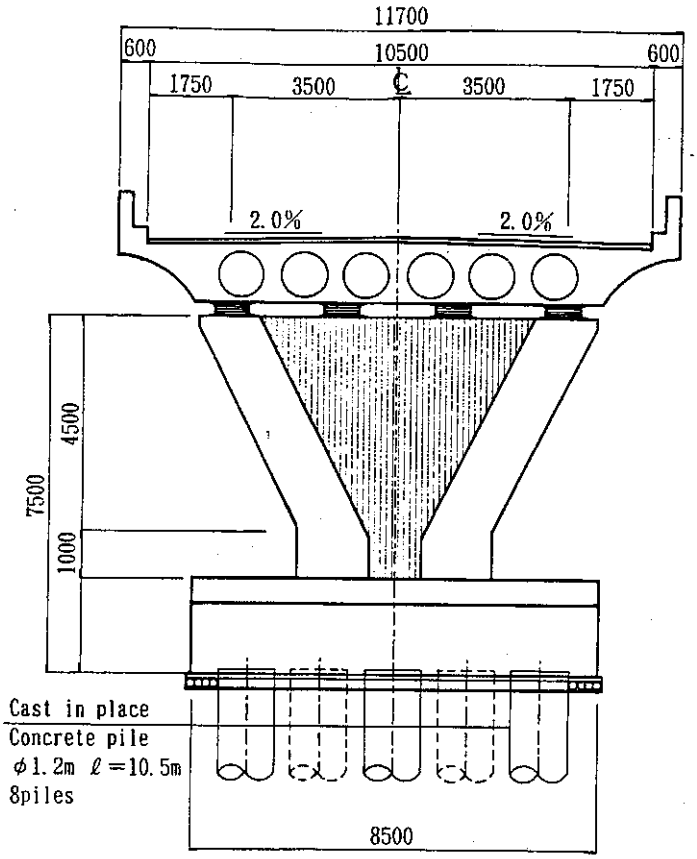

Figure 12. View of the standard Bridge Pier Configuration

Table 3. Substructure Stiffness Table

Bridge Pier Number	P_0	$P_1 \sim P_5$	$P_6 \sim P_{10}$	$P_{11} \sim P_{14}$	$P_{15} \sim P_{18}$	$P_{19} \sim P_{23}$	$P_{24} \sim P_{28}$	P_{29}
Elastic Stiffness of the Substructure Kca(tf/m)	17,700	16,500	24,100	16,000	14,000	17,700	19,100	20,00
Yield Stiffness of the Substructure Kyn(tf/m)	17,500	15,600	23,000	15,600	12,700	15,600	16,400	19,70

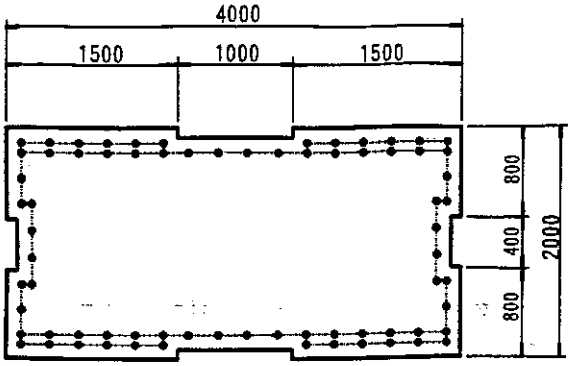

Principal Reinforcing Bar in the Bridge Axis Direction D25
Principal Reinforcing Bar in the Transverse Direction D16

Figure 13. Cross Section and Reinforcing Bar Arrangement in the Bridge Pier

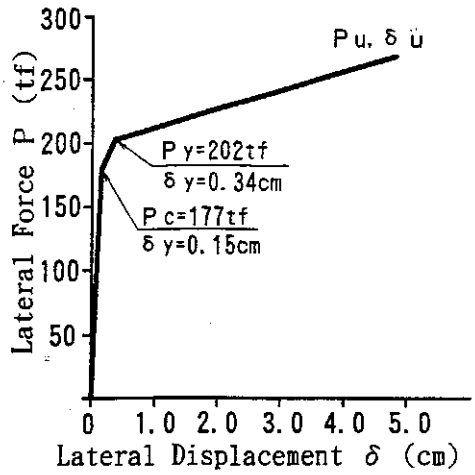

Figure 14. P-δ Curve of the Wall

MENSHIN DESIGN

The final design requirements for the Menshin design of this bridge have not yet been finalized, because the basic items dealt with during the planning and design of this bridge will be determined in accordance with the deliberations and guidance of a supervisory committee. This committee is now considering the many items described above. This section presents details on all the studies of Menshin design conducted up until this time, but is still incomplete.

1) Basic Design Policies

The basic design policies will conform to the provisions of the "highway bridge specifications", items that are peculiar to Menshin design and those that are not prescribed by the highway bridge specifications will conform to the "Manual for the Menshin Design of Highway Bridges (draft)" from the Public Works Research Center, and such design will be conducted in accordance with policies approved by the supervisory committee.

2) Menshin Design

The balance between the thermal change deformation lateral forces and the seismic lateral forces is one of the major items. A trial computation of the stiffness of the Menshin devices is carried out in order to avoid a situation in which the shape of the substructure would be determined by the forces applied during a temperature change deformation. For example, thermal lateral force and other lateral forces during an earthquake shown on Figure 15(A) and (B) shows the relation between the natural period of vibration and the thermal lateral force and seismic lateral force. Figure (A) shows the relationship with thermal lateral force generated in a typical pier, and Figure (B) shows the relationship with the bearing's relative displacement during an L1 and L2 earthquake. These trial computations clarify that if Menshin devices are not to be determined by temperature change deformation, the natural period during an L2 level earthquake would have to be between 1.3 and 1.4 seconds. Various other studies are now in progress. As a reference, Table 4 presents the results of Menshin design trial computations in a case where the natural period is 1.4 seconds.

Table 4. Menshin Design Trial Calculation Results Table (T = 1.4 sec.)

(Lateral Force and Stiffness are all Values Per Single Bridge Pier)

Bridge Pier Number				P_1	P_2~P_5	P_6~P_{10}	P_{11}~P_{21}	P_{22}~P_{23}	P_{24}~P_{25}	P_{26}~P_{29}	P_{30}
Number of Piers				1	4	5	11	2	2	2	1
Bearing Shape	Lateral		A×B (cm)	55×55	75×80	75×80	75×80	75×80	75×80	75×80	55×55
	Rubber Laminated		Σte (cm)	14.0	12.8	12.8	12.8	12.8	12.8	12.8	14.0
Normal Conditions	Lateral Displacement of Bearing		Uo (cm)	8.2	7.2	5.1	3.4	2.0	4.9	6.9	8.2
	Lateral Shear Force of Bearing (slow-rate)		Fs (tf)	62.7	121.7	86.2	57.5	33.8	82.8	116.7	62.7
	Effective Cross Section Area of the Rubber		A_{Ro} (cm^2)	2242.	4849	5013	5145	5304	5028	4872	2037
	Check of Bearing Stress	σmax(kgf/cm^2)[<80]		61.1	57.1	50.5	49.2	47.7	55.1	56.9	67.3
Seismic Coefficient Method Level	Design Displacement of Menshin Devices		U_B (cm)	4.61	4.18	4.20	4.23	3.94	3.96	3.96	4.50
	Effective Design Displacement of Menshin Devices		U_{Be} (cm)	3.23	2.93	2.94	2.96	2.76	2.78	2.78	3.15
	Equivalent Stiffness of Menshin Devices		K_B (tf/m)	521.8	1201.2	1197.2	1192.4	1247.7	1243.5	1243.5	529.8
	Equivalent Stiffness of synthesizing the Menshin Device and Substructure		Kr (tf/m)	1923	4017	4024	4033	3935	3942	3942	1907
	Equivalent Damping Ratio of Menshin Devices		h_B	0.251	0.254	0.254	0.254	0.257	0.257	0.257	0.252
	Allotment Rate of Horizontal Foce		η	0.0694	0.1449	0.1452	0.1455	0.1419	0.1422	0.1422	0.0688
	Natural period of the Bridge		T (sec)	0.898							
	Equivalent Damping Ratio of the Bridge		h	0.220							
	Lateral Seismic Coefficient		Kh	0.25							
	Design Lateral seismic Force		F (tf)	96	201	201	202	197	197	197	95
	Extent of Superstructure Displacement		Ur (tf)	5.002							
Ultimate Lateral Strength Level During an Earthquake	Design Displacement of Menshin Devices		U_B (cm)	32.79	30.86	31.19	31.58	29.42	30.57	30.57	32.64
	Effective Design Displacement of Menshin Devices		U_{Be} (cm)	22.95	21.60	21.84	22.10	20.59	21.40	21.40	22.85
	Equivalent Stiffness of Menshin Devices		K_B (tf/m)	199.3	441.1	440.9	440.7	442.0	441.2	441.2	199.3
	Effective Equivalent Stiffness of Menshin Devices		K_{Be} (tf/m)	208.0	458.7	457.6	456.3	464.3	459.8	459.8	208.2
	Equivalent Stiffness of synthesizing the Menshin Device and Substructure		Kre (tf/m)	787	1631	1646	1662	1569	1619	1619	784
	Equivalent Damping Ratio of Menshin Devices		h_{Be}	0.142	0.146	0.145	0.143	0.151	0.147	0.147	0.142
	Allotment Rate of Horizontal Foce		η	0.0693	0.1444	0.1458	0.1476	0.1379	0.1430	0.1430	0.0690
	Natural period of the Bridge		T (sec)	1.405							
	Equivalent Damping Ratio of the Bridge		he	0.135							
	Lateral Seismic Coefficient		khc	0.68							
	Design Lateral seismic Force		F (tf)	261	545	550	557	520	540	540	260
	Extent of Superstructure Displacement		Ur (cm)	34.568							

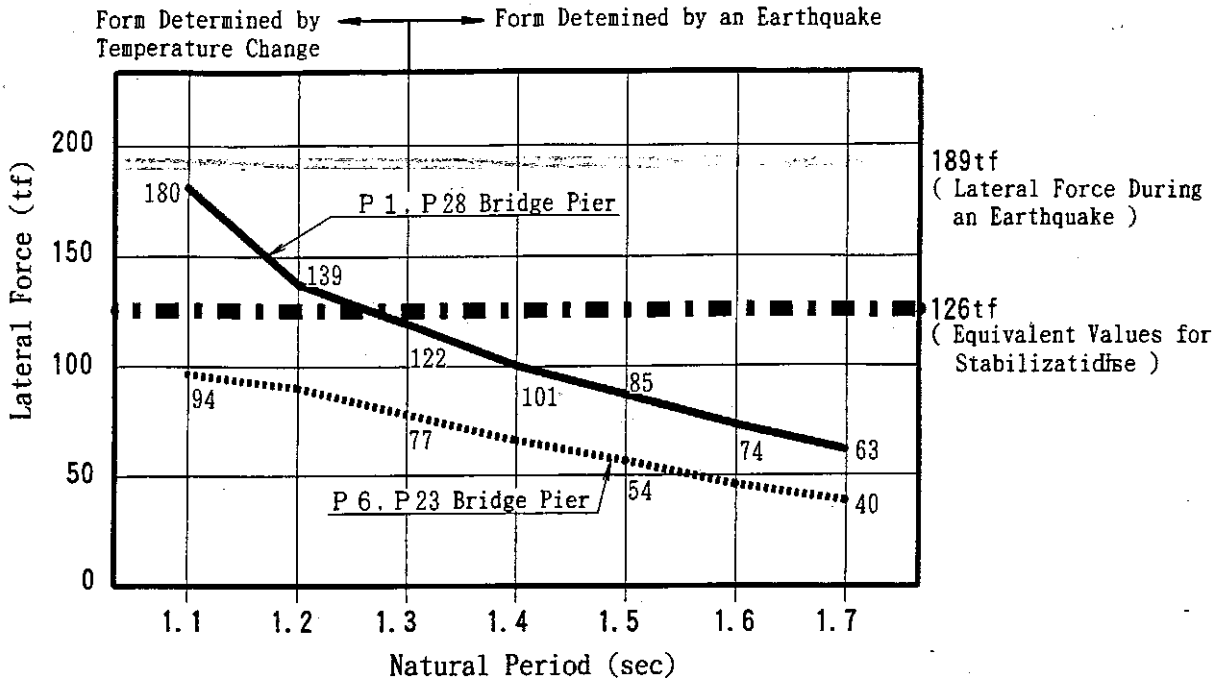

(A) Relationship Between the Natural Period of the Bridge and Thermal Lateral Force

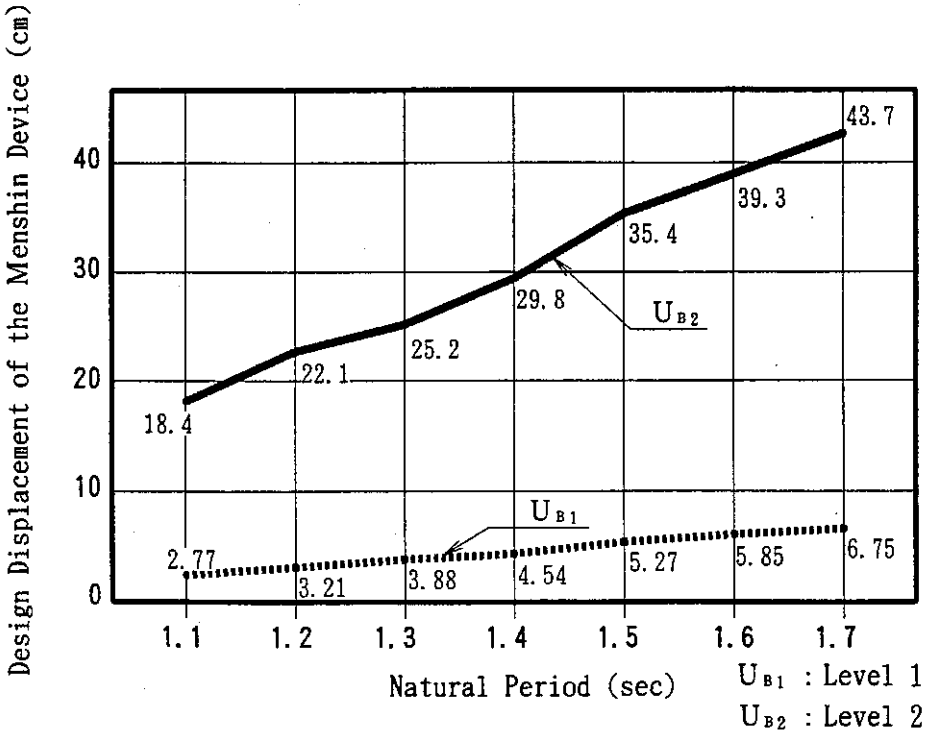

(B) Relationship Between the Natural Period of the Bridge and the Design Bearing Displacement

Figure 15.

CONCLUSION

At this time, the planning and design of this project has reached the stage where a variety of studies are in progress in accordance with basic policies. Because the examples introduced in this paper represent only part of the overall research effort, reports on details of these studies, the results of final design work, and the actual construction will be made available at every opportunity.

We would like to express our deep appreciation to members of the supervisory committee and to other related organizations for their generous cooperation and guidance with this project.

REFERENCES

1) Public Works Research Institute: Manual for Menshin Design of Highway Bridges (Drafts), Technical Note of Public Works Research Institute, Vol. 60, December, 1992.
2) Japan Road Association: Specifications for Highway Bridge , Part I to V, February, 1990.
3) Civil Engineering Journal, Vol. 35, No. 1, January, 1993.